Cite this article
Karagöz Y, Balcı Ö, Gezer O, Köten H and Işın Ö (2021)
Performance and emissions of spark-ignition engines fuelled with petrol and methane.
Proceedings of the Institution of Civil Engineers – Energy **174(4)**: 156–169,
https://doi.org/10.1680/jener.19.00055

Research Article
Paper 1900055
Received 13/06/2019;
Accepted 01/10/2020;
Published online 11/01/2021

Keywords: energy conservation/environment/pollution

Energy

ice Publishing

Performance and emissions of spark-ignition engines fuelled with petrol and methane

Yasin Karagöz PhD
Assistant Professor, Department of Mechanical Engineering, Engineering Faculty, Istanbul Medeniyet University, Kadıköy, Istanbul, Turkey (corresponding author: yasin.karagoz@medeniyet.edu.tr)

Özgün Balcı MSc
Research Assistant, Automotive Division, Department of Mechanical Engineering, Mechanical Engineering Faculty, Yildiz Technical University, Yildiz, Besiktas, Istanbul, Turkey

Onur Gezer MSc
Research Assistant, Automotive Division, Department of Mechanical Engineering, Mechanical Engineering Faculty, Yildiz Technical University, Yildiz, Besiktas, Istanbul, Turkey

Hasan Köten PhD
Associate Professor, Department of Mechanical Engineering, Engineering Faculty, Istanbul Medeniyet University, Kadıköy, Istanbul, Turkey

Övün Işın PhD
Assistant Professor, Automotive Division, Department of Mechanical Engineering, Mechanical Engineering Faculty, Yildiz Technical University, Yildiz, Besiktas, Istanbul, Turkey

Diesel engines using compression ignition are increasingly prohibited in cities due to increased environmental concerns. This could lead to greater use of low-powered spark-ignition (SI) engines in hybrid electrical cars. Using alternative fuels is important for SI engines. In this research study, performance and in-cylinder pressure data were collected from petrol- and methane-fuelled SI engines. A theoretical engine model was then verified using experimental data. The theoretical results for methane and petrol were finally compared for different engine speeds. The theoretical model used a combustion model and a chemical kinetics model to compare the effects of methane and petrol on engine performance and emissions at different engine speeds. Thanks to the high knock resistance of methane, the most suitable ignition advance value was decided for the methane-fuelled simulation by considering the maximum thermal efficiency to limit assumed reductions in indicated thermal efficiency and indicated mean effective pressure compared to previous studies. A slight reduction in nitrous oxides and carbon monoxide emissions was observed when using methane at full load.

Notation

a	vibe parameter
EP_i	specific emission value of relevant gases (g/kWh)
EV_i	relevant gases amount in proportion to total exhaust gases
LHV_f	lower heating values of fuels (petrol or methane) (kJ/kg).
M_i and M_{exh}	molar mass, of relevant gases and exhaust gases respectively (kg/kmol).
m	shape parameter
$\dot{m}_f$	mass flow rates of fuels (petrol or methane) (kg/s)
$\dot{m}_{exh}$ and $\dot{m}_{int}$	mass flow rates of exhaust gases and intake air, respectively (g/h)
N_i	indicated engine power (kW)
n	engine speed (r/min)
P	measured in-cylinder pressure (Pa)
P_{mi}	mean indicated pressure (Pa)
Q	total fuel heat input
$\dot{Q}$	heat release rate (HRR) (J/°CA) and k is the working mixture polytrophic index
V	instant cylinder volume (m^3) calculated in Equation 1
V_H	cylinder displacement (m^3)
W_i	indicated work of the engine per cycle (J)
$(W_R)_{P,B}$	propagated uncertainty for either precision error $(W_R)_P$, or systematic (bias) error $(W_R)_B$ functions
$w_1, w_2,...w_n$	corresponding uncertainties of the variables
$x_1, x_2,...,x_n$	measured variables
α	crank angle (degree)
α_0	crank angle at the beginning of combustion
$\Delta\alpha_c$	combustion duration
ε	compression ratio of the engine
λ	ratio of crank radius to connecting rod length

1. Introduction

In recent years, not only has the number of diesel vehicles increased, but also the rate of growth has increased in the vehicle park (EEA, 2017). This situation causes environmental concerns, especially due to nitrous oxides and particulate matter (EEA, 2016a). To mitigate the problem, the use of diesel vehicles in urban centres have been restricted at various locations around the world (EPCA, 2017; TfL, 2016).

Currently, research and development have been accelerated on electric-motor-powered vehicles, but there are still issues such as insufficient battery storage capacity, limited availability of

charging stations and excessive charging times in this scenario. Improving these mentioned problems for electric vehicles requires time (EEA, 2016b). The reduction in fossil fuel reserves, in parallel with the world's increasing energy demand, is also a serious problem. For this reason, switching to biofuels instead of conventional fuels in road transport has substantial importance in terms of both energy supply and emission control (Costagliola *et al*., 2016; Iodice and Senatore, 2016; Iodice *et al*., 2018).

Therefore, power-pack systems with low-power spark-ignition (SI) engines operated with alternative fuels are predicted to become widespread. Using these alternative gas-powered power units, which can be used in serial or parallel with electric motors in hybrid vehicles, provides a great advantage, especially in urban traffic conditions.

Methane is an environmental-friendly fuel for internal combustion engines, with a low carbon/hydrogen ratio and wide flammability limits (Pan *et al*., 2018). Additionally, it is known that methane is a gaseous fuel and this situation enhances the homogeneity of the air–fuel mixture. Also, methane has benefits in terms of emissions thanks to the high hydrogen content (Pan *et al*., 2018). Some further physicochemical properties of petrol and methane fuels can be found in Table 1. Natural gas contains methane in high proportion and methane does not contain carbon-to-carbon chemical bonds (Lyu *et al*., 2017). Currently, the use of methane in SI engines is a realistic approach, since natural gas is a more economic fuel than diesel fuel (Hu *et al*., 2017). Studies that have used methane and natural gas in SI engines are summarised in the next paragraphs.

Irimescu *et al*. (2014) investigated the performance parameters of methane and petrol in an SI engine experimentally. This study shows that if the ignition advance is optimised when using the methane as an energy source, the combustion efficiency increases compared to petrol. Both fuel types have similar characteristics in terms of heat losses. Gharehghani *et al.* (2015) used a four-cylinder naturally aspirated engine in their experimental study and they compared compressed natural gas (CNG) and petrol. According to results obtained from this study, the engine power output increased but thermal efficiency slightly decreased when petrol was used as fuel. Higher exergy efficiency has been achieved with the use of CNG. Tahir *et al.* (2015) observed in their study that the use of CNG causes lower in-cylinder pressure values and lower power output than petrol. The authors claimed that the volumetric efficiency decreases when using CNG. When using CNG, in-cylinder pressure reduction up to 20%, heat losses reduction up to 23% and output power reduction up to 18.5% were observed compared to petrol.

Table 1. Comparison of properties of petrol and methane

Parameter	Petrol	Methane
Formula	C_4–C_{12}	CH_4
C/H ratio: %	0.56	0.25
Molecular weight: kg/kmol	98	16
Density of standard conditions: kg/m^3	720	0.67
Auto-ignition temperature: °C	350	540
Research octane number	92	125
Stoichiometric air–fuel ratio	14.6	17.24
Quenching distance: mm	2.02	2.03
Flammability limit: vol %	5.3/14	1.4/7.6
Laminar burning velocity: m/s	0.45	0.43

Source: Pan *et al*. (2018)

In some studies, natural gas was used in liquid form, which is known as LNG. Chen *et al.* (2017) were interested in the methane content of LNG fuel in their experimental study. This study used two different fuel compositions which included 93 and 99% methane proportionally. The study was carried out with three different compression ratios and ignition advance values. According to results, the blend which includes 99% methane has the highest knock resistance. At full load condition, the brake-specific fuel consumption (BSFC) had the lowest value by using 99% methane fuel, because methane has higher knock resistance and ignition timing can be advanced.

In some studies, hydrogen and methane blends were used in SI engines. Moreno *et al.* (2012) examined the effect of fuel content by blending hydrogen and methane at different rates for a naturally aspirated SI engine. The hydrogen concentration in the fuel blend was increased up to 50% volumetrically. It was observed that as the methane ratio decreased, NO_x (oxides of nitrogen) emissions and brake thermal efficiency (BTE) decreased. Akansu *et al*. (2007) used a four-cylinder engine in their experimental study and they blended hydrogen and methane in different ratios volumetrically. The studies were conducted under 2000 r/min (revolutions per minute) engine speed and constant engine load. They found that BTE and nitrogen oxide (NO) increased, and hydrocarbons (HCs), carbon monoxide and carbon dioxide decreased as the hydrogen concentration increased.

In some studies, methane was used as a fuel blend with some HCs such as propane, butane and so on for SI engines. Montoya *et al*. (2016) used a four stroke, single cylinder SI engine, the compression ratio of which can be adjusted between 4 and 18, and they used methane–hydrogen and propane–hydrogen blends as fuel. From this study, it has been seen that methane–hydrogen blends have higher knock resistance and higher thermal efficiency than propane–hydrogen blends. Amirante *et al.* (2017) used a single-cylinder, port injection, SI engine in their study. They used pure methane,

pure propane, a propane–methane mixture and natural gas under a stoichiometric air–fuel ratio and full load condition at 2000, 3000 and 4000 r/min engine speeds. The ratio of methane in the methane–propane mixture varied between 10 and 40%. It is evident from results of their study that changes in the rate of propane and methane have a significant effect on performance and emission parameters. While the propane ratio increases, the complete combustion improves and indicated mean effective pressure (IMEP) and NO_x increase due to higher in-cylinder temperatures.

In some studies, biogas fuel has been used in SI engines. Subramanian *et al.* (2013) compared methane-enriched biogas (93% methane) and base CNG (89.14% methane) fuel in an SI engine for the Indian driving cycle (MIDC). In terms of fuel economy, there is no significant difference between enriched biogas and base CNG fuel. Also, no visible difference was observed in carbon dioxide emissions per kilometre. Using methane-enriched biogas fuel in an SI engine decreases carbon monoxide, HC and NO_x emissions slightly.

Even though many studies on methane have been carried out in the literature, none of the studies has used a single-cylinder, extremely light-duty engine, which can be used in a small power-pack as a range extender for hybrid systems in the near future. Although there are many studies about different alternative gaseous fuel mixtures in the literature, in this study the use of pure methane fuel was investigated, because using natural gas in SI engines is a feasible, realistic and economical method. It has also been emphasised that small-power (old technology carburetted) engines can be calibrated and converted to run on methane fuel, taking into account the maximum indicated thermal efficiency (ITE) map and appropriate ignition advance, by means of an attached injection system, quickly and experimentally verified by a numerical model. First the experimental studies with petrol and methane fuels were completed, then the mathematical model was verified. Also, the optimum ignition advance was determined considering maximum ITE values for methane fuel. Finally, the acquired combustion characteristics (in-cylinder pressure, heat release rate (HRR)), emission and performance values were compared with neat petrol and methane fuels.

2. Material and methods

Figure 1 shows a schematic view of the engine test set-up in the laboratory. The figure shows that the test bench consists of an SI engine loaded by a dynamometer and external resistive load banks, sensors which were installed to collect intake air flow, in-cylinder pressure, crank position, engine speed, fuel consumption and emission data and a post-processing system.

The experimental process was conducted at 2650 and 3400 r/min engine speeds. The experimental set-up and theoretical models are built to run at stoichiometric conditions for petrol and methane fuels. Stoichiometric air–fuel ratios of the petrol and methane were assumed as 14.6 and 17.24, respectively.

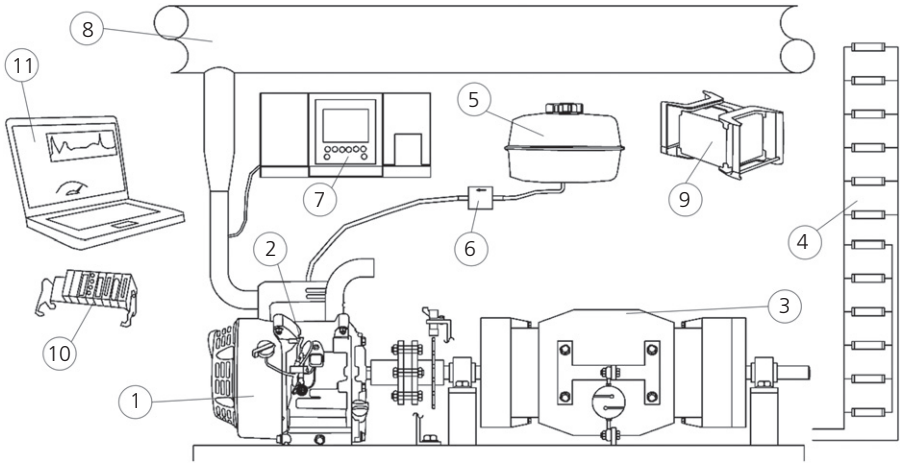

1. Test engine, 2. pressure sensor, 3. dynamometer, 4. external resistive load banks, 5. gasoline tank, 6. gasoline flowmeter, 7. exhaust gas analyser, 8. exhaust ventilation system, 9. KiBox combustion analyser, 10. NI data-acquisition device, 11. personal computer for data recording and post processing

Figure 1. Schematic explanation of the experimental set-up

2.1 Experimental set-up

A single-cylinder, four-stroke, 270 cm^3, air-cooled, naturally aspirated SI engine was used in the experiments. The engine was loaded by an alternative current dynamometer.

The sensor group includes a mass flowmeter to measure intake air mass flow rate, a spark plug-type Kistler 6118B in-cylinder pressure transducer, an incremental type encoder to evaluate crank position and engine speed data, a miniature oval gear-type fuel flowmeter to determine the fuel consumption and an AVL Digas 4000 gas analyser to measure exhaust gases emissions.

In the experimental tests, the data that were collected from the in-cylinder pressure sensor were sent to the Kistler KiBox combustion analyser device and recorded for post-processing.

For the determination of specific exhaust gases emissions, mass flow rate of intake air data and emission data were used and the method specified in the German Mechanical Engineering Industry Association (VDMA) exhaust emission legislation for gas engines was used in calculations.

2.2 Engine specifications and dynamometer features

In this experimental study, a naturally aspirated, air-cooled, four-stroke, single-cylinder, SI, Honda engine which has 270 cm^3 engine swept volume was used. Further information about the engine and dynamometer is given in Table 2.

2.3 SI engine model

A 270 cm^3, single-cylinder SI engine used in the engine tests was mathematically modelled with the help of AVL Boost software, which reaches the result with both a one-dimensional (quasi-dimensional) model and a zero-dimensional model. The intake and exhaust lines are determined one-dimensionally by using the finite-element method, and in-cylinder behaviours are determined according to zero-dimensional thermodynamic approaches. The friction model in the programme was run to obtain friction mean efective pressure depending on the speed and indicated pressure. The piston and bore diameter, stroke, compression ratio, connecting rod length and the clearance distance that may lead to blow-by leakage are entered to determine the combustion chamber geometry, and local loss coefficients were entered in the programme.

Table 2. Engine specifications and dynamometer features

Engine specifications	
Engine manufacturer	Honda
Number of cylinders	1
Compression ratio	8.5:1
Cooling	Air
Bore × stroke: mm	77 × 58
Cylinder volume: cm^3	270
Net power: kW	6.3/3600 r/min
Recommended speed range: r/min	2000–3500
Aspiration	Natural
Dynamometer features	
Power: kVA kW	8

The parameters of the engine model and Vibe 2 Zone combustion model, which was used in this study, were determined by using experimentally obtained data. Two-zone vibe is a model that is preferred in many academic studies. In the two-zone vibe modelling, the combustion chamber is divided into two regions, one of which the flame has not yet reached and the other is the combusted area. AVL Boost software contains a sub-programme BURN which determines the HRR values considering the heat transfer (Rimkus *et al.*, 2015). The K-epsilon model was chosen as the turbulence model. The K-epsilon model gives very good results in determining both the regions where the flame has not yet reached and the flame propagation regions (Sjerić *et al.*, 2016). This also reveals the co-operation compatibility with the two-zone vibe combustion model. Laminar flame velocity was modelled in accordance with the Metghalchi and Keck correlation, and turbulence burning velocity was modelled in accordance with the Bradley correlation, as in the study by Gupta and Abdel-Gayed (2015). The heat-transfer model is built according to Woschni; this method is highly preferred in the literature and instantly solves heat transfer.

Petrol and methane fuels were chosen for simulations from classic species set-up of AVL Boost software, which is used through a programme to calculate combustion kinetics and intermediary reactions, and hence emissions. Figure 2 depicts

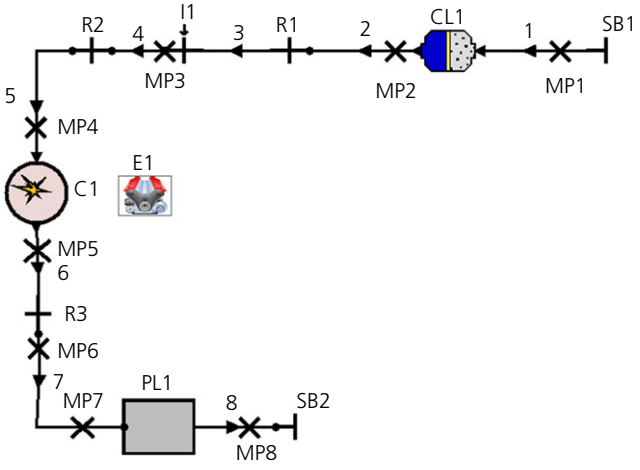

Figure 2. View of AVL Boost single-cylinder mathematical engine model

the schematic view of the theoretical model of the test engine. The Vibe 2 Zone model in the study was used in order to get fast results and to be a method in which methane calibration can be performed quickly.

3. Data reduction

IMEP can be calculated as shown in Equation 3 (Heywood, 1988) by using indicated engine work as given in Equation 2 (Heywood, 1988).

$$1. \quad V = \frac{V_H}{2}\left[(1-\cos\alpha)+\frac{\lambda}{4}(1-\cos 2\alpha)\right]+\frac{V_H}{\varepsilon-1}$$

$$2. \quad W_{\mathrm{i}} = \int_0^{720} P\mathrm{d}V$$

$$3. \quad P_{\mathrm{mi}} = \frac{W_i}{V_H}$$

where V is the instant cylinder volume (m^3) calculated in Equation 1, V_H is the cylinder displacement (m^3), λ is the ratio of crank radius to connecting rod length, α is the crank angle (CA) (degrees), ε is the compression ratio of the engine, W_i is the indicated work of the engine per cycle (J), P_{mi} is the mean indicated pressure (Pa) and P is measured in-cylinder pressure (Pa).

ITE can be calculated as seen in Equation 5 (Bauer and Forest, 2001) by using the indicated torque value, which is stated in Equation 4.

$$4. \quad N_i = \frac{W_i \times n}{60 \times 2}$$

$$5. \quad \mathrm{ITE} = \frac{N_i}{\dot{m}_{\mathrm{f}} \times \mathrm{LHV_f}}$$

where N_i is the engine power (kW), n is the engine speed (r/min), ITE is the indicated thermal efficiency, $\dot{m}_{\mathrm{f}}$ is the mass flow rates of fuels (petrol or methane) (kg/s) and $\mathrm{LHV_f}$ is the lower heating value (LHV) of fuels (petrol or methane) (kJ/kg).

HRR calculations from the experimental data were realised as shown in Equation 6 (Egnell, 1998).

$$6. \quad \dot{Q} = \frac{k}{k-1}P\frac{\mathrm{d}V}{\mathrm{d}\theta}+\frac{k}{k-1}V\frac{\mathrm{d}P}{\mathrm{d}\theta}$$

where $\dot{Q}$ is the HRR (J/°CA) and k is the working mixture polytrophic index.

Besides, the Vibe 2 Zone approximation, which was used as a combustion model of theoretical engine model in this study, calculates HRR values by using the vibe function as shown in Equations 7–9 (AVL, 2013).

$$7. \quad \frac{\mathrm{d}x}{\mathrm{d}\alpha} = \frac{\alpha}{\Delta\alpha_{\mathrm{c}}}(m+1)y^m \mathrm{e}^{-a\,y^{(m+1)}}$$

$$8. \quad \mathrm{d}x = \frac{\mathrm{d}Q}{Q}$$

$$9. \quad y = \frac{\alpha-\alpha_0}{\Delta\alpha_{\mathrm{c}}}$$

where Q is the total fuel heat input, α is the CA, α_0 is the CA at the beginning of combustion, $\Delta\alpha_{\mathrm{c}}$ is the combustion duration, m is the shape parameter, a is the vibe parameter, which is equal to 6.9 for complete combustion. The parameters of the vibe function are approximated by also using the mass fraction burned equation of vibe.

The exhaust emissions were measured using gas analyser by volume while executing the tests. Mass flow rate of total exhaust gases can be calculated by adding measured flow rate of intake air and consumed fuel as seen in Equation 10 (VDMA, 2017). Consequently, specific emissions can be obtained as shown in Equation 11 (VDMA, 2017).

$$10. \quad \dot{m}_{\mathrm{exh}} = \dot{m}_{\mathrm{int}} + \dot{m}_{\mathrm{f}}$$

$$11. \quad \mathrm{EP}_i = \mathrm{EV}_i \times \frac{M_i}{M_{\mathrm{exh}}} \times \frac{\dot{m}_{\mathrm{exh}}}{N_i}$$

where $\dot{m}_{\mathrm{exh}}$ and $\dot{m}_{\mathrm{int}}$ are the mass flow rates of exhaust gases and intake air, respectively (g/h), EP_i is the specific emission value of relevant gases (g/kWh), EV_i is the relevant gases amount in proportion to the total exhaust gases (by volume for carbon monoxide and by particle count for total unburned hydrocarbon (THC) and NO_x) and M_i and M_{exh} are the molar masses of relevant gases and exhaust gases, respectively (kg/kmol).

Kline and McClintock analysis (Kline and McClintock, 1953) determined the total propagated uncertainty of the precision

and systematic (bias) errors measurement as

$$12. \quad (W_R)_{\mathrm{P,B}} = \left[\left(\frac{\partial R}{\partial x_1} w_1\right)^2 + \left(\frac{\partial R}{\partial x_2} w_2\right)^2 + \cdots + \left(\frac{\partial R}{\partial x_n} w_n\right)^2\right]^{1/2}$$

Hence, the total uncertainty W_R is computed with

$$13. \quad W_R = \sqrt{(W_R)_{\mathrm{P}}^2 + (W_R)_{\mathrm{B}}^2}$$

where $(W_R)_{\mathrm{P,B}}$ denotes the propagated uncertainty for either precision error $(W_R)_{\mathrm{P}}$ or systematic (Bias) error $(W_R)_{\mathrm{B}}$ functions. x_1, x_2,…,x_n are the measured variables and w_1, w_2,…w_n are the corresponding uncertainties of the variables.

4. Test procedure

In the experimental part of this study, a 270 cm^3 SI engine was run at 2650 and 3400 r/min engine speeds at full load condition. All tests were run at stoichiometric air–fuel ratio. In-cylinder pressure data, fuel consumption and emissions were measured and collected at these working conditions. In the experiments, a spark plug-type pressure sensor was located in the middle of the combustion chamber due to constructive restrictions. Hence, the collected pressure data were highly exposed to pressure fluctuation in the combustion chamber. To avoid fluctuant data, an embedded filter was used in the Kistler combustion analyser device. Then, the theoretical model for SI engines was created by using collected data and determined combustion model parameters.

4.1 Petrol-fuelled validation

For validation of the mathematical model with petrol, in-cylinder pressure and HRR data acquired from the experimental study, were compared and examined at 2650 and 3400 r/min engine speed.

Figures 3 and 4 show the variations of in-cylinder pressure and normalised HRR values, which were obtained from experimental results and mathematically modelled studies with petrol at 2650 r/min. Figures 5 and 6 also show these values at an engine speed of 3400 r/min. The maximum in-cylinder pressure values were obtained as 36.11 bar for the experimental method and 35.17 bar for simulation results, respectively. The maximum normalised HRR values at 2650 r/min engine speed were 0.0358 1/°CA and 0.0329 1/°CA. At 2650 and 3400 r/min engine speeds, errors between the experimental and theoretical data were 2.6 and 8.1% (according to the experimental data) in terms of maximum in-cylinder pressure and normalised HRR, respectively. At 3400 r/min engine speed, maximum in-cylinder pressure values obtained from the

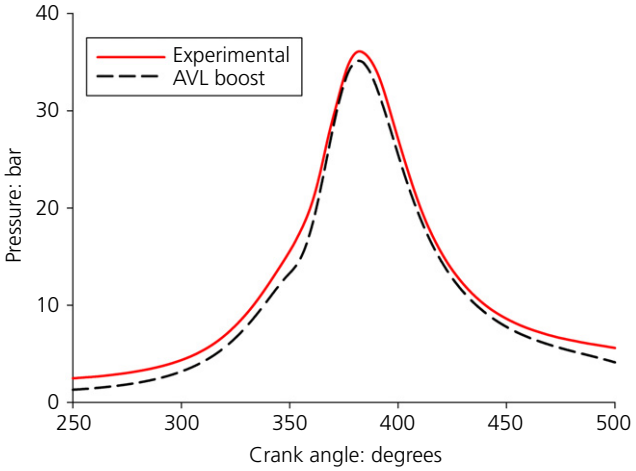

Figure 3. In-cylinder pressure variations of experimental and theoretical data at 2650 r/min engine speed with petrol

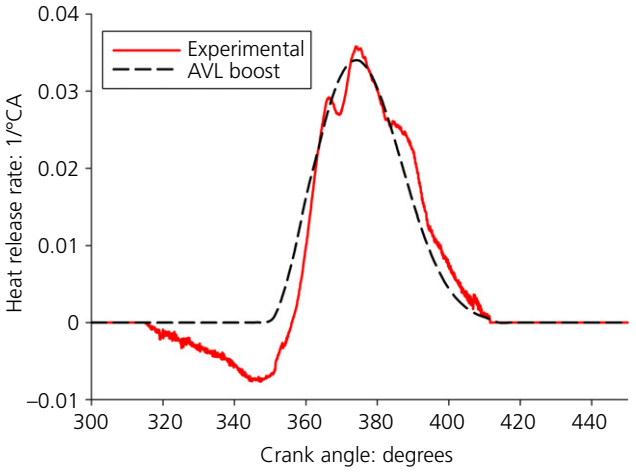

Figure 4. Normalised heat release variations of experimental and theoretical data at 2650 r/min engine speed with petrol

experiments and simulations were 28.35 and 27.46 bar, normalised HRR values were 0.0246 and 0.0267 1/°CA, and percentage errors were 3.1 and 8.5%, respectively.

As mentioned before, in-cylinder pressure data were obtained by using a spark plug-type pressure transducer, which was located in the middle of the combustion chamber, hence highly exposed to pressure fluctuations. In contrast, the KiBox combustion analyser device has its own filtering process during pressure data acquisition. However, the derivative of pressure term in Equation 6 causes additional fluctuations in HRR variations, in spite of filtered pressure data (Deng *et al.*, 2013; Geo *et al.*, 2019; İlhak *et al.*, 2020; Yu *et al.*, 2020).

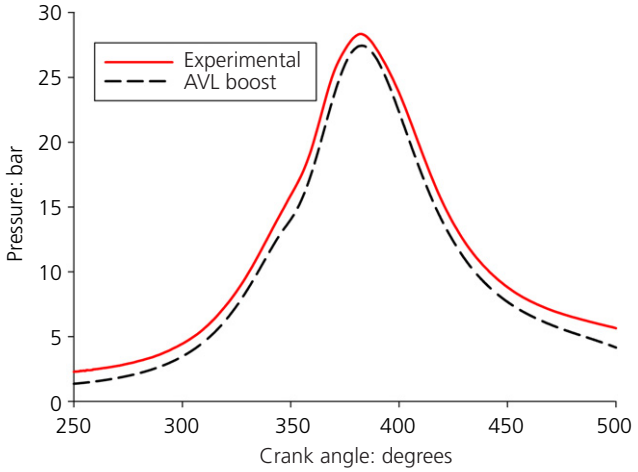

Figure 5. In-cylinder pressure variations of experimental and theoretical data at 3400 r/min engine speed with petrol

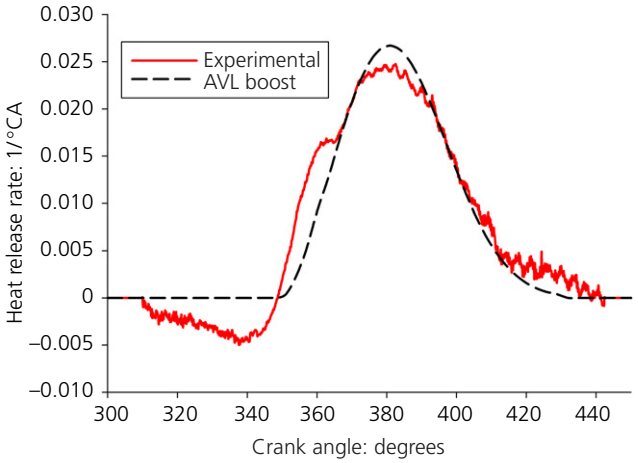

Figure 6. Normalised heat release variations of experimental and theoretical data at 3400 r/min engine speed with petrol

The above-mentioned slightly rough HRR variations, which are seen in Figures 4 and 6, were not filtered in order to conserve original characteristics of the heat release variations.

The variations shown in Figures 3–6 have good agreement in terms of their fundamental features, such as the beginning and the end of HRR, maximum in-cylinder pressure, maximum HRR and in general terms. Therefore, it is concluded that the above-mentioned results adequately satisfy the validation of the theoretical model.

4.2 Methane-fuelled validation

For validation of the mathematical model with methane fuel, in-cylinder pressure data which were acquired from experimental study, were compared and examined at 3400 r/min engine speed.

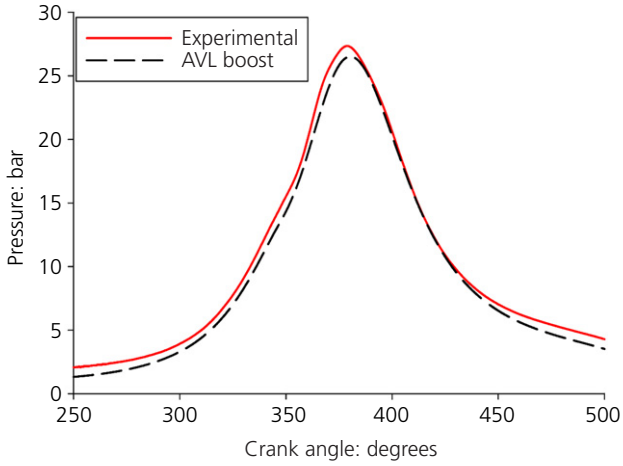

Figure 7. In-cylinder pressure variations of experimental and theoretical data at 3400 r/min engine speed with methane fuel

Figure 7 shows the variations of in-cylinder pressure which were obtained from experimental results and mathematically modelled studies by using methane at 3400 r/min. The maximum in-cylinder pressure values were obtained as 27.35 bar for experimental method and 26.52 bar for simulation results, respectively. The error rates between the experimental data and theoretically obtained data were 3.0% (according to the experimental data) in terms of maximum in-cylinder pressure.

In Figures 3, 5 and 7, the proportional difference between the theoretical and experimental in-cylinder pressure values is high at the beginning of compression. Although the pressure data received through the cylinder has very low values during intake and at the beginning of the compression strokes, the pressure sensor that was used in the tests is designed for high-pressure measurements. Therefore, in the mentioned regions, the error ratio is relatively large in proportion to the pressure values obtained from the simulations. This difference is predicted not to cause a fault in the examination of the engine performance, emissions and combustion processes, since it occurs at the intake stroke.

As seen from Figures 3–7, the pressure and HRR data of the experimental results and theoretical model results are overlapped. Additionally, other performance and emission values of experimental results and theoretical model results are given in Tables 3 and 4. The maximum error ratio occurred at THC emission with 8.32% for 3400 r/min engine speed with petrol. Consequently, it is seen that these compared values are close enough to confirm the theoretical model.

Table 3. Petrol fuelled model validation parameters and error values

Parameter	Experimental (2650/3400 r/min)	Simulation	Error: %
Maximum pressure: bar	36.11/28.35	35.17/27.46	2.6/3.1
ITE: %	25.25/21.94	25.04/21.69	0.82/1.16
IMEP: bar	9.46/8.88	9.55/8.76	–0.99/1.31
Carbon monoxide: g/kWh	933/1309	941/1282	–0.86/2.06
THC: g/kWh	1.44/1.16	1.51/1.26	–4.78/–8.60
NO_X: g/kWh	1.55/1.20	1.54/1.22	1.05/–1.76

Table 4. Methane fuelled model validation parameters and error values

Parameter	Experimental	Simulation	Error: %
Maximum pressure: bar	27.35	26.52	3.0
ITE: %	19.98	19.68	1.48
IMEP: bar	7.81	7.93	–1.58
Carbon monoxide: g/kWh	1254	1232	1.74
THC: g/kWh	1.49	1.57	–5.12
NO_X: g/kWh	1.08	1.06	2.21

Table 5. Measurement accuracies and the calculated uncertainties

Parameter	Device	Accuracy
Engine speed	Incremental encoder	± 5 r/min
In-cylinder pressure	Kistler 6118B	± 0.3 bar
Petrol flow rate	Biotech VZS-005	± 1% (of reading)
Methane flow rate	New-Flow TLF	± 1% (F.S.)
Carbon monoxide	AVL Digas 4000	0.01% vol.
THC	AVL Digas 4000	1 ppm
NO_x	AVL Digas 4000	1 ppm
Calculated results		Uncertainty value
Indicated specific energy consumption		± 0.68 ÷ 0.79%

Experiments were executed in Yildiz Technical University, Internal Combustion Engines Laboratory. The test equipment measurement uncertainties are shown in Table 5.

4.3 Simulations

After the validation, engine performance and emission values were obtained from simulation results for petrol at 2650, 2900, 3150, 3400 and 3650 r/min engine speeds. Later, simulations were run for methane fuel at the same engine speeds and engine performance parameter values and emission characteristics were compared for two different fuels at stoichiometric working conditions.

Since methane has relatively lower flame speed and higher knock resistance than petrol, simulations were run with higher ignition advance for methane in order to provide maximum ITE.

5. Results and discussion

In the first step, performance and emission values of the SI engine were obtained experimentally, then the theoretical model was validated by the experimental results. Afterwards, all the results for both petrol and methane fuels were obtained theoretically. Also, the results of petrol and methane fuels were compared and examined in terms of in-cylinder pressure, normalised HRR, ITE, IMEP and indicated specific carbon monoxide emission, indicated specific THC emission and indicated specific NO_x emissions.

5.1 Pressure and HRR variations

Figure 8 shows in-cylinder pressure variations for petrol and methane fuels at each engine speed. As a result of data which were obtained from the theoretical model, the maximum pressure values by using methane fuel at 2650, 2900, 3150, 3400 and 3650 r/min the engine speeds drop from 35.17 to 32.07 bar, from 32.70 to 30.22 bar, from 30.00 to 28.58 bar, from 27.46 to 26.52 bar and from 25.62 to 24.75 bar, respectively.

In methane fuel simulations, the decrease in in-cylinder pressure was limited by using higher ignition advance with the help of the high knock resistance of methane. While working with methane fuel, reductions in maximum pressure values can be explained by the fact that the LHV of methane on volume basis and the volumetric energy content in the cylinder are lower than that of gasoline fuel (Thurnheer *et al*., 2009).

For petrol and methane fuels, the normalised HRR variations were compared as seen in Figure 9 for five different engine speed values. Similarly, by using methane fuel rather than petrol, the maximum normalised HRR values were decreased from 0.0329 to 0.0298 1/°CA, from 0.0291 to 0.0280 1/°CA, from 0.0270 to 0.0260 1/°CA, from 0.0267 to 0.0243 1/°CA and from 0.0234 to 0.0230 1/°CA.

The highest decrease in in-cylinder maximum pressure value was detected as 8.8% and the highest decrease in normalised HRR was detected as 9.4% for using methane compared to petrol.

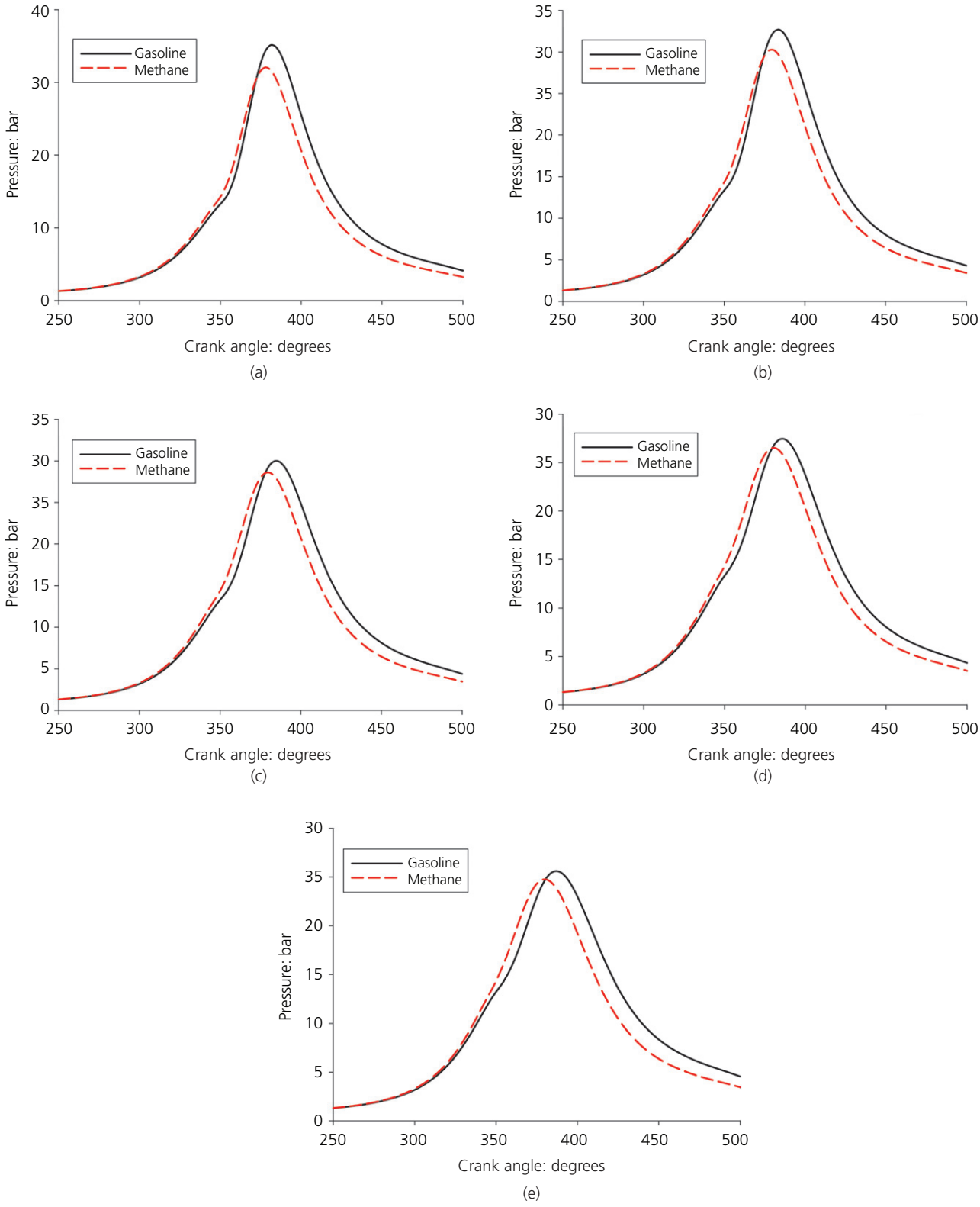

Figure 8. In-cylinder pressure variation comparisons of petrol and methane in different engine speeds: (a) 2650 r/min, (b) 2900 r/min, (c) 3150 r/min, (d) 3400 r/min, (e) 3650 r/min

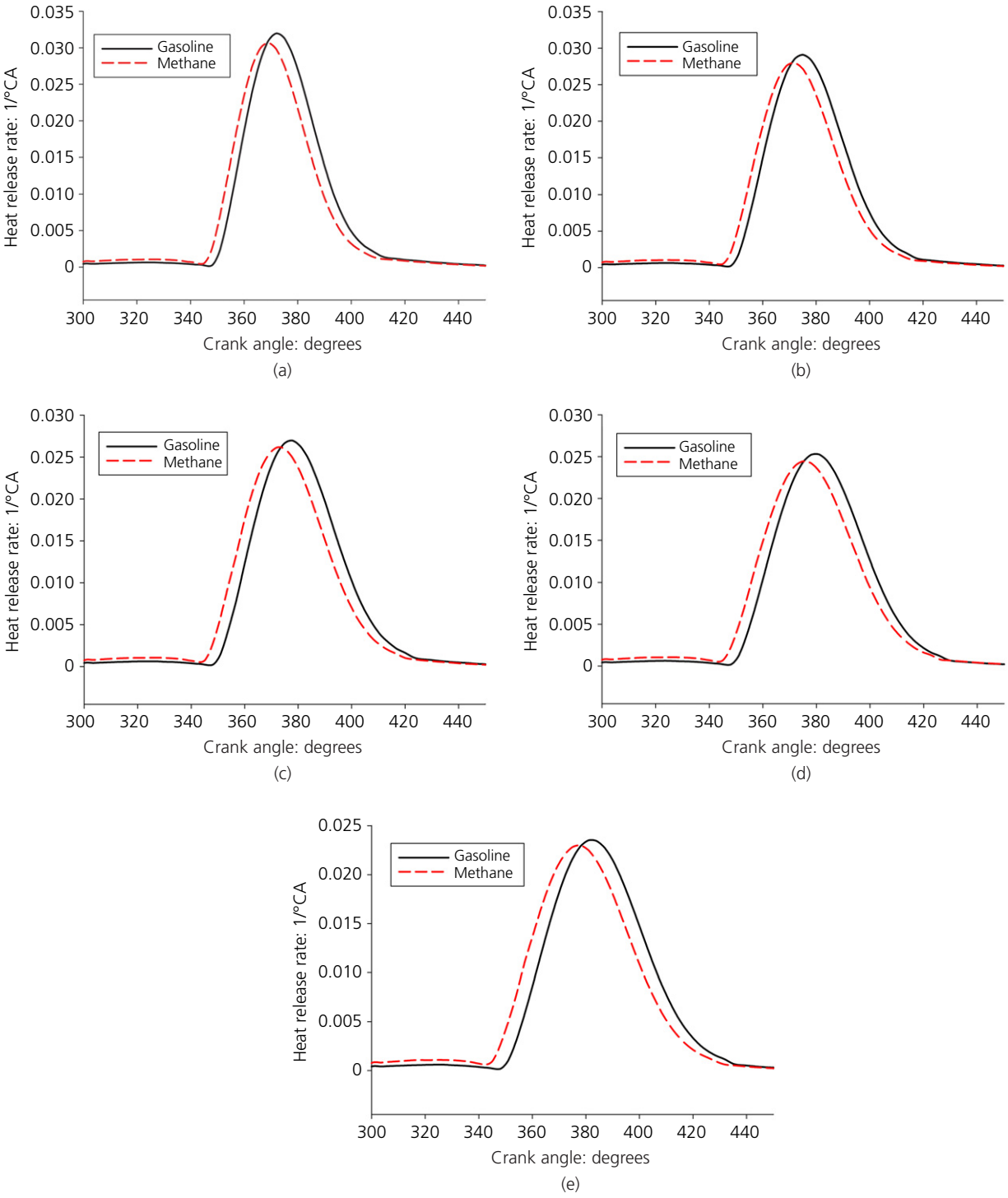

Figure 9. Normalised HRR variation comparisons of petrol and methane in different engine speeds: (a) 2650 r/min, (b) 2900 r/min, (c) 3150 r/min, (d) 3400 r/min, (e) 3650 r/min

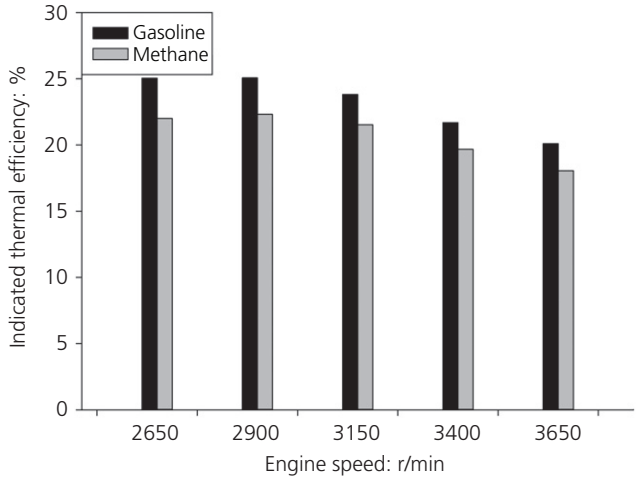

Figure 10. Comparisons of ITE of petrol and methane

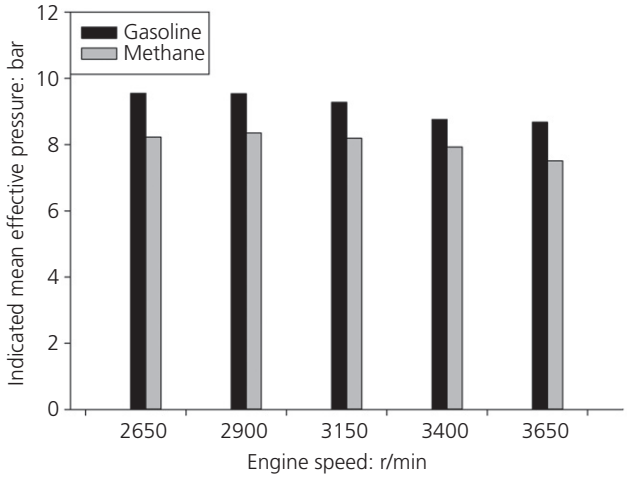

Figure 11. Comparisons of IMEP of petrol and methane

The maximum normalised HRR values were decreased by using methane fuel since methane has a relatively lower burning velocity than petrol. Also, methane combustion occurs more slowly than for petrol, and hence the duration of methane combustion is higher than the duration of petrol combustion.

5.2 Indicated thermal efficiency

Figure 10 shows a comparison of ITE values for petrol and methane at five different engine speeds. The ITE values obtained at the mentioned engine speeds (2650, 2900, 3150, 3400 and 3650 r/min) were observed as 25.04–22.01%, 25.07–22.32%, 23.82–21.53%, 21.69–19.68%, 20.11–18.06% for petrol and methane fuels, respectively.

The reduction in thermal efficiency by using methane causes low flame velocity. Since the duration of methane combustion is longer than for gasoline fuel (Di Iorio *et al*., 2016; Irimescu, 2013), the petrol combustion process occurs closer to the ideal constant volume cycle. Thanks to the high knock resistance of methane, ignition timing advanced slightly to limit thermal efficiency drop (Chen *et al*., 2017).

5.3 Indicated mean effective pressure

Figure 11 shows the IMEP values which were obtained from the simulations. IMEP values decreased between 9.47 and 13.82% by using methane as fuel. According to the theoretical results for methane fuel, energy output value decreased per cycle and lower IMEP values were obtained due to LHV on volume basis and lower energy density per unit volume of methane gas.

5.4 Carbon monoxide

Air–fuel ratio is one of the most important parameters for carbon monoxide emissions. As mentioned earlier, simulations have been run at nearly stoichiometric air–fuel ratio condition for both petrol and methane fuel. Figure 12 shows the specific carbon monoxide emissions at different engine speeds, which were obtained from the theoretical model for petrol and methane fuels. While working with methane as fuel, there is a slight decrease in specific carbon monoxide emissions for all engine speeds. The maximum drop occurred as 5.42% by using methane fuel at 3650 r/min engine speed. Although in peak in-cylinder pressure and in-cylinder temperature values were reduced by using methane, the low C/H ratio of methane causes slight reduction in specific carbon monoxide emission values. Knowing that methane is the major component of CNG, Putrasari *et al.* (2015) claimed that the lower C/H ratio

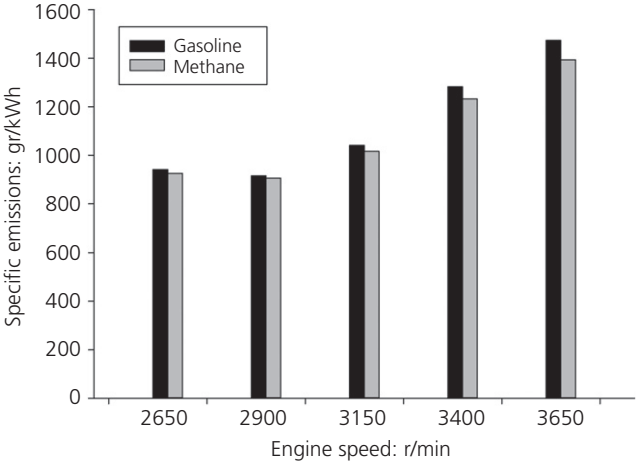

Figure 12. Specific carbon monoxide emission comparisons of petrol and methane

causes lower carbon monoxide emission in their study when using CNG as the fuel. Under these conditions, the lower carbon monoxide emissions with methane usage can be attributed to the lower C/H ratio and lower carbon content of methane fuel. Besides, local rich mixture regions and chemical equilibrium values due to macro mixture irregularities can be seen as a source of carbon monoxide generated as emissions.

5.5 Total unburned HCs

Specific THC emissions, which were acquired from different engine speeds for methane and petrol, can be seen in Figure 13. The graph shows that specific THC emission values increased between 16.56 and 28.52% for all engine speeds with methane fuel simulation. The maximum rise in THC emission occurred at 3650 r/min engine speed and it increased from 1.40 to 1.80 g/kWh, which equals an increase of 28.52%.

THC emissions are sensitive to many constructive factors (combustion chamber surface and volume ratio, blow-by effect, narrow volumes etc.) and operating conditions (engine load, ignition advance, regime temperature, engine speed). As can be seen in Figure 13, the THC emission drops as the engine speed increases due to improved macro scale mixture properties and flame extinction zones reduced with an increase in combustion chamber turbulence level (Szwaja *et al.*, 2018). The duration of combustion gets practically longer in terms of CA as the engine speed increases further. Thus, the improvement rate of THC decreases due to insufficient time for combustion before the chamber volume expands. When the engine speed exceeds a certain value, this effect becomes dominant and leads THC emissions to show an increasing trend (Duc *et al.*, 2019). Moreover, increase of both frictional and inertial losses with increasing engine speed cause more apparent increase in specific THC emissions in comparison to THC emissions in parts per million (ppm) (Suiuay *et al.*, 2020). The THC results, which are shown in Figure 13, are in agreement with the studies of Duc *et al.* (2019) and Asfar and Al-Azzam (2001).

The quenching distance, which is the most important parameter for THC emission, is nearly the same for both fuels (Pan *et al.*, 2018). Meanwhile, due to the low flame velocity of methane, maximum in-cylinder temperature values drop, which is the main reason for the high THC emission for methane simulations.

5.6 Nitrous oxides

Emissions of oxides of nitrogen, which need high-cost aftertreatment systems, are very harmful to human health (Wang *et al.*, 2018). It is very important to keep a check on NO_x, which are emitted from internal combustion engines. Specific NO_x emissions at different engine speeds for petrol and methane fuel are shown in Figure 14. In this study, specific NO_x emissions decreased from 1.54 to 1.39 g/kWh at 2650 r/min engine speed. Similarly nitrogen oxides emission values decreased from 1.40 to 1.24 g/kWh at 2900 r/min, from 1.32 to 1.15 g/kWh at 3150 r/min, from 1.22 to 1.06 g/kWh at 3400 r/min and from 1.16 to 0.99 g/kWh at 3650 r/min engine speed by using methane fuel. The reduction in specific NO_x emissions at 2650, 2900, 3150, 3400 and 3650 r/min engine speeds by using methane as fuel were 9.41, 11.36, 13.10, 12.76 and 14.72%, respectively.

The NO_x emissions are largely dependent on in-cylinder temperature values (Guardiola *et al.*, 2017). Hence, low maximum pressure and temperature values due to the low flame speed

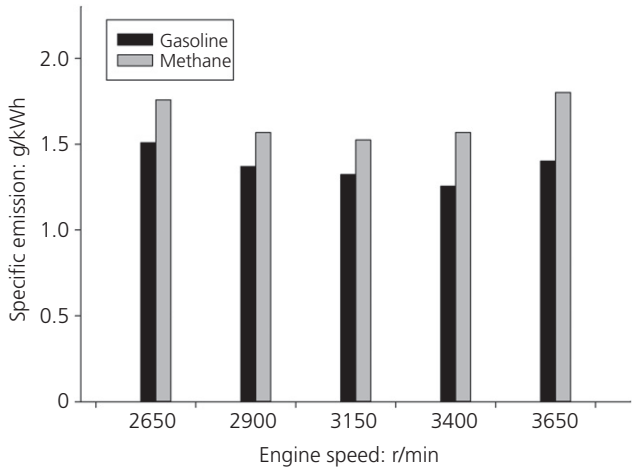

Figure 13. Specific THC emission comparisons of petrol and methane

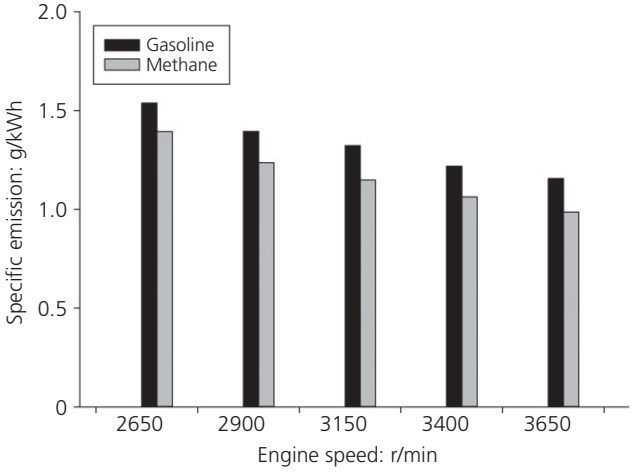

Figure 14. Specific NO_x emission comparisons of petrol and methane

(Di Iorio *et al.*, 2016) and low energy content of methane explain a dramatic decrease in NO_x emissions.

6. Conclusion

In this study, petrol and methane fuels were investigated and compared at full engine load, stoichiometric condition and different engine speeds (2650–3650 r/min). First, the SI engine was experimentally tested and performance, emission values and combustion characteristics were obtained with petrol at 2650 and 3400 r/min engine speeds and with methane at 3400 r/min engine speed. Second, a theoretical model was developed and validated with the petrol- and methane-fuelled experimental results. Finally, methane and petrol SI engine simulations were compared with each other and the results obtained are summarised as given below.

- Maximum in-cylinder pressure and maximum normalised HRR values were decreased up to 8.8 and 9.4%, respectively, by using methane as fuel in the SI engine. The reason is that methane has lower energy density, lower flame velocity and lower energy content on volume basis than petrol.
- ITE and IMEP values were reduced up to 12.1 and 13.82%, respectively, by using methane. This is because methane has low flame velocity and low LHV on volume basis.
- Carbon monoxide emissions slightly improved (up to 5.4%) by using methane. The reason is the low C/H ratio of methane fuel. However, a dramatic increase (up to 28.5%) in THC emissions could not be prevented. This is because methane has a lower flame velocity than petrol. An unprecedented improvement (up to 14.7%) was obtained in NO_x emissions. The reason is that low in-cylinder pressure and low in-cylinder temperature values were obtained during methane-fuelled SI engine operation.
- Currently, the use of CNG and LNG in public transportation buses and LPG in passenger cars is becoming widespread. Provided that the applicable conditions are met, the performance advantage will become prominent, due to the higher thermal capacity of methane. At the same time, compared to liquid fuels, the mixture provides a great deal of homogeneity because it is injected in the gas phase. Thus, liquid inertia, evaporation process and other factors that worsen the macro scale mixture formation are eliminated and a more homogeneous mixture can be obtained.
- In future studies it will be useful to examine the post-combustion emission reduction methods for methane and petrol operating conditions. Due to different combustion performances and different values of the chemical composition and the temperature of the exhaust gas due to their thermal values, studies aiming to optimise the current performance and performance of the closed-loop three-way catalytic converters for changing fuel conditions will contribute to a strong alternative to conventional fuels.

Acknowledgements

This research was supported by Tubitak (Scientific and Technological Research Council of Turkey) with 1512 project (project number: 2150175). The authors are also indebted to Şahin Metal A.Ş. and Erin Motor for providing them with test apparatus and equipment donation. Balcı has been financially supported by TUBITAK 2228-B program.

REFERENCES

Akansu SO, Kahraman N and Çeper B (2007) Experimental study on a spark ignition engine fuelled by methane–hydrogen mixtures. *International Journal of Hydrogen Energy* **32(17)**: 4279–4284.

Amirante R, Distaso E, Di Iorio S *et al.* (2017) Effects of natural gas composition on performance and regulated, greenhouse gas and particulate emissions in spark-ignition engines. *Energy Conversion and Management* **143**: 338–347.

Asfar KR and Al-Azzam R (2001) Engine performance using vaporizing carburetor. *Energy Conversion and Management* **42(6)**: 755–761.

AVL (2013) *Theory AVL BOOST v2013.2*, Edition 11/2013. AVL LIST GmbH, Graz, Austria.

Bauer CG and Forest TW (2001) Effect of hydrogen addition on the performance of methane-fueled vehicles. Part I: effect on SI engine performance. *International Journal of Hydrogen Energy* **26(1)**: 55–70.

Chen Z, Zhang F, Xu B, Zhang Q and Liu J (2017) Influence of methane content on a LNG heavy-duty engine with high compression ratio. *Energy* **128**: 329–336.

Costagliola MA, Prati MV, Florio S *et al.* (2016) Performances and emissions of a 4-stroke motor cycle fuelled with ethanol/gasoline blends. *Fuel* **183**: 470–477.

Deng B, Fu J, Zhang D *et al.* (2013) The heat release analysis of bio-butanol/gasoline blends on a high speed SI (spark ignition) engine. *Energy* **60**: 230–241.

Di Iorio S, Sementa P and Vaglieco BM (2016) Analysis of combustion of methane and hydrogen–methane blends in small DI SI (direct injection spark ignition) engine using advanced diagnostics. *Energy* **108**: 99–107.

Duc KN, Duy VN, Hoang-Dinh L, Viet TN and Le-Anh T (2019) Performance and emission characteristics of a port fuel injected, spark ignition engine fuelled by compressed natural gas. *Sustainable Energy Technologies and Assessments* **31**: 383–389.

EEA (European Environment Agency) (2016a) *Air Quality in Europe*. EEA, Copenhagen, Denmark, Report number 28/2016.

EEA (2016b) *Electric Vehicles in Europe*. EEA, Copenhagen, Denmark, Report number 20/2016.

EEA (2017) *Monitoring CO_2 Emissions from New Passenger Cars and Vans in 2016*. EEA, Copenhagen, Denmark, Report number 19/2017.

Egnell R (1998) Combustion diagnostics by means of multizone heat release analysis and NO calculation. *SAE Transactions* **107(4)**: 691–710.

EPCA (Environment Pollution (Prevention and Control) Authority) for the National Capital Region (2017) *Comprehensive Action Plan for Air Pollution Control*. EPCA, Delhi, India, Report number 70.

Geo VE, Godwin DJ, Thiyagarajan S, Saravanan CG and Aloui F (2019) Effect of higher and lower order alcohol blending with gasoline on performance, emission and combustion characteristics of SI engine. *Fuel* **256**: 115806.

Gharehghani A, Hosseini R, Mirsalim M and Yusaf TF (2015) A comparative study on the first and second law analysis and performance characteristics of a spark ignition engine using either natural gas or gasoline. *Fuel* **158**: 488–493.

Guardiola C, Martín J, Pla B and Bares P (2017) Cycle by cycle NO_x model for diesel engine control. *Applied Thermal Engineering* **110**: 1011–1020.

Gupta A and Abdel-Gayed R (2015) Qualitative governing approach of a spark ignition engine using exhaust gas recirculation. *Energy Procedia* **66**: 97–100.

Heywood JB (1988) *Internal Combustion Engine Fundamental*. McGraw-Hill Inc., New York, NY, USA.

Hu M, Huang W, Cai J and Chen J (2017) The evaluation on liquefied natural gas truck promotion in Shenzhen freight. *Advances in Mechanical Engineering* **9(6)**: 1687814017705065.

İlhak Mİ, Doğan R, Akansu SO and Kahraman N (2020) Experimental study on an SI engine fueled by gasoline, ethanol and acetylene at partial loads. *Fuel* **261**: 116148.

Iodice P and Senatore A (2016) Atmospheric pollution from point and diffuse sources in a National Interest Priority Site located in Italy. *Energy & Environment* **27(5)**: 586–596.

Iodice P, Langella G and Amoresano A (2018) Ethanol in gasoline fuel blends: effect on fuel consumption and engine out emissions of SI engines in cold operating conditions. *Applied Thermal Engineering* **130**: 1081–1089.

Irimescu A (2013) Comparison of combustion characteristics and heat loss for gasoline and methane fueling of a spark ignition engine. *Proceedings of the Romanian Academy, Series A* **14(2)**: 161–168.

Irimescu A, Vasiu G and Tordai GT (2014) Performance and emissions of a small scale generator powered by a spark ignition engine with adaptive fuel injection control. *Applied Energy* **121**: 196–206.

Kline SJ and McClintock FA (1953) Describing uncertainties in single-sample experiments. *Mechanical Engineering* **75(1)**: 3–8.

Lyu M, Zhang C, Bao X, Song J and Liu Z (2017) Effects of the substitution rate of natural gas on the combustion and emission characteristics in a dual-fuel engine under full load. *Advances in Mechanical Engineering* **9(12)**: 1687814017747158.

Montoya JPG, Amell AA and Olsen DB (2016) Prediction and measurement of the critical compression ratio and methane number for blends of biogas with methane, propane and hydrogen. *Fuel* **186**: 168–175.

Moreno F, Muñoz M, Arroyo J *et al.* (2012) Efficiency and emissions in a vehicle spark ignition engine fueled with hydrogen and methane blends. *International Journal of Hydrogen Energy* **37(15)**: 11495–11503.

Pan J, Li N, Wei H, Hua J and Shu G (2018) Experimental investigations on combustion acceleration behavior of methane/gasoline under partial load conditions of SI engines. *Applied Thermal Engineering* **139**: 432–444.

Putrasari Y, Praptijanto A, Nur A, Wahono B and Santoso WB (2015) Evaluation of performance and emission of SI engine fuelled with CNG at low and high load condition. *Energy Procedia* **68**: 147–156.

Rimkus A, Žaglinskis J, Rapalis P and Skačkauskas P (2015) Research on the combustion, energy and emission parameters of diesel fuel and a biomass-to-liquid (BTL) fuel blend in a compression-ignition engine. *Energy Conversion and Management* **106**: 1109–1117.

Sjerić M, Taritaš I, Tomić R *et al.* (2016) Efficiency improvement of a spark-ignition engine at full load conditions using exhaust gas recirculation and variable geometry turbocharger–numerical study. *Energy Conversion and Management* **125**: 26–39.

Subramanian KA, Mathad VC, Vijay VK and Subbarao PMV (2013) Comparative evaluation of emission and fuel economy of an automotive spark ignition vehicle fuelled with methane enriched biogas and CNG using chassis dynamometer. *Applied Energy* **105**: 17–29.

Suiuay C, Laloon K, Katekaew S *et al.* (2020) Effect of gasoline-like fuel obtained from hard-resin of Yang (*Dipterocarpus alatus*) on single cylinder gasoline engine performance and exhaust emissions. *Renewable Energy* **153**: 634–645.

Szwaja S, Ansari E, Rao S *et al.* (2018) Influence of exhaust residuals on combustion phases, exhaust toxic emission and fuel consumption from a natural gas fuelled spark-ignition engine. *Energy Conversion and Management* **165**: 440–446.

Tahir MM, Ali MS, Salim MA *et al.* (2015) Performance analysis of a spark ignition engine using compressed natural gas (CNG) as fuel. *Energy Procedia* **68**: 355–362.

TfL (Transport for London) (2016) *Taxi and Private Hire Action Plan*. Transport for London, London, UK.

Thurnheer T, Soltic P and Eggenschwiler PD (2009) SI engine fuelled with gasoline, methane and methane/hydrogen blends: heat release and loss analysis. *International Journal of Hydrogen Energy* **34(5)**: 2494–2503.

VDMA (VDMA Engines and Systems) (2017) *Exhaust Emission Legislation Diesel and Gas Engines*. VDMA, Frankfurt, Germany.

Wang ZX, Wang LW, Gao P, Yu Y and Wang RZ (2018) Analysis of composite sorbents for ammonia storage to eliminate NO_x emission at low temperatures. *Applied Thermal Engineering* **128**: 1382–1390.

Yu X, Li G, Dong W *et al.* (2020) Numerical study on effects of hydrogen direct injection on hydrogen mixture distribution, combustion and emissions of a gasoline/hydrogen SI engine under lean burn condition. *International Journal of Hydrogen Energy* **45(3)**: 2341–2350.